

Production of two simultaneously trapped Bose-Einstein condensates by RF coupling in a TOP trap

J. L. Martin, C. R. McKenzie, N. R. Thomas, D. M. Warrington and A. C. Wilson

Department of Physics, University of Otago, PO Box 56, Dunedin, New Zealand

(February 8, 2020)

A radio frequency (RF) transition is used to convert a pure ^{87}Rb Bose-Einstein condensate in the $F = 2, m_F = 2$ state to a mixture of $F = 2, m_F = 2$ and $F = 2, m_F = 1$ states, which are simultaneously confined by a time-averaged orbiting potential (TOP) magnetic trap. We show that the nature of this coupling process is strongly influenced by the presence of the time varying field of the TOP trap, and complicated by the presence of multiple Zeeman substates. In particular, the effective Rabi frequency associated with the applied RF field is not constant across the spatial extent of the cloud leading to loss of spatial control in atom-laser output coupling and ‘averaging out’ of Rabi oscillations. Further a time-varying detuning can give rise to complex spatial structures.

PACS Number(s): 03.75.Fi,05.30.Jp,32.80.Pj,42.55.-f

The development of atom-laser output coupling schemes and techniques for coupling single state Bose-Einstein condensates (BEC) into two-component condensates have been the subject of many recent experimental studies. The motivation behind these studies is the development of practical output couplers and the investigation of interactions within condensate mixtures. For these experiments, robust and controllable production of different output states is essential. Two-component condensates have been produced using sympathetic cooling [1], two photon (RF and microwave) transitions [2], and in optical dipole traps [3]. The latter allows simultaneous trapping of all the states within a hyperfine manifold. Several output coupling schemes have been demonstrated experimentally: simple RF output coupling [4–6], optically induced Bragg diffraction [7,8] and Josephson tunneling [9]. Of the six research groups who performed these studies, four used time-averaged orbiting potential (TOP) traps [10]. This letter extends the study of RF output coupling to include the production of two simultaneously trapped condensates with controllable relative populations. However, the degree of control is strongly influenced by the dynamics of the TOP trap. We find the presence of the time varying magnetic field of the TOP trap can significantly increase the apparent spectral width of the applied RF field, which in turn limits the overall spatial control of the coupling region. We also find that the large quadrupole gradient of the TOP trap gives rise to a large change in the effective Rabi frequency across the cloud, thereby limiting our control of relative populations. Finally, spatio-temporal coupling can give rise to complex spatial structures and phase profiles.

Our experimental procedure has been described in [6]. We start with a ^{87}Rb Bose-Einstein condensate in the $|F = 2, m_F = 2\rangle$ state, confined in a TOP trap with radial quadrupole field gradient $B'_q = 200 \text{ G cm}^{-1}$ and bias field $B_{\text{TOP}} = 4 \text{ G}$. We then apply an RF coupling field with polarization perpendicular to the plane of rotation of the TOP field. The effect of this field is to induce

transitions between adjacent m_F states in the $F = 2$ hyperfine manifold, and hence the initially pure $|2, 2\rangle$ condensate state becomes a mixture of the five possible m_F states. By changing the frequency, duration and magnitude of the coupling field different admixtures of the manifold states can be generated. Note that states $|2, -1\rangle$ and $|2, -2\rangle$ are high field seeking and therefore actively repelled from the trap, and state $|2, 0\rangle$ being essentially magnetically insensitive is untrapped; hence these states will be present in the trapping region for only a few milliseconds after the coupling pulse. Once the coupling field has been applied we separate the trapped components by removing the trapping potential and 1 ms later applying a magnetic field gradient which introduces a Stern-Gerlach separation. The different magnetic sub-states ($|2, 2\rangle$ and $|2, 1\rangle$) become easily resolvable after about 5 ms. Although the probing pulse is tuned on resonance with the $|2, 2\rangle$ state, the population of the $|2, 1\rangle$ state is also accurately determined since the 50 μs probing pulse (in a 4 G bias field) leads to rapid optical pumping into the $|2, 2\rangle$ state. This gives us effective resonant probing of both condensate m_F states. Typical results of this process are shown in Fig. 1.

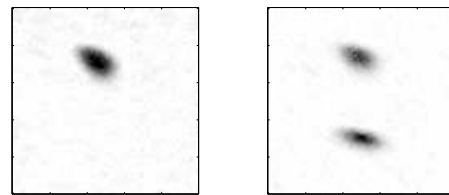


FIG. 1. (a) An image of a Bose condensate without any coupling field applied. (b) A similar condensate after application of an RF field tuned to the centre of the trap with magnitude 72 mG applied for 32 μs . The individual images are 250 μm along each axis and are taken after a 5 ms time-of-flight through the inhomogeneous magnetic field.

To analyze this coupling process, it is helpful conceptually to first consider the case of a static magnetic trap,

such as a Ioffe-Pritchard (I-P) configuration. When an RF field is applied to couple atoms into other states, the static magnetic field gradient gives rise to a static but spatially varying detuning Δ . To calculate the linewidth of a pulse of duration τ_{pulse} we must consider the relative effects of the pulse spectral width and power broadening (note that the natural linewidth of an RF transition is insignificant in comparison). The pulse spectral width is given by

$$\Gamma_{\text{spectral}} = \frac{2\pi}{\tau_{\text{pulse}}}, \quad (1)$$

and the power broadening (for $m_F = 2$) by [11]

$$\Gamma_{\text{power}} = \frac{g_F \mu_B B_{\text{rf}}}{\sqrt{2}\hbar}, \quad (2)$$

where B_{rf} is the magnetic field amplitude of the RF coupling field. These two linewidths combine to give an intrinsic linewidth associated with the RF pulse

$$\Gamma_{\text{pulse}} = \sqrt{\Gamma_{\text{spectral}}^2 + \Gamma_{\text{power}}^2}. \quad (3)$$

We now include the effects of a time varying magnetic field. In a typical TOP trap significant angular change in the orientation of the bias field will occur during even a short RF pulse (e.g. with a bias field rotating at $\omega_{\text{TOP}} = 7$ kHz, a 10 μs pulse corresponds to a 25° change). The effect of this rotation is to introduce time dependence to the already spatially varying detuning. As the quadrupole field rotates about the centre of the cloud the detuning at any fixed point varies sinusoidally with time. In addition, the rotation of the field introduces a spatially dependent transit time broadening of the transition linewidth. Effectively, the available interaction time is reduced from τ_{pulse} to τ_{transit} by the time varying detuning. This transit time broadening, Γ_{transit} , depends on the distance r from the axis of rotation of the TOP field (in our case the z-axis) and Γ_{pulse}

$$\Gamma_{\text{transit}} = 2\pi r \omega_{\text{TOP}} \frac{\omega'_q}{\Gamma_{\text{pulse}}}, \quad (4)$$

where ω'_q is the radial gradient of the RF transition frequency (arising from the Zeeman shift associated with the quadrupole field gradient B'_q) given by

$$\omega'_q = g_F B'_q \frac{\mu_B}{\hbar}. \quad (5)$$

By careful choice of experimental parameters, one might hope to ignore the complications introduced by the rotating field. This could be achieved, for example, by broadening the RF transition so that the coupling rate is essentially the same for all atoms. In our experiment, the transition frequency gradient is 14 kHz μm^{-1} and our condensate width is ≈ 30 μm , giving a change in the transition frequency across the spatial extent of the cloud of 420 kHz. Therefore, in order for the coupling field to be insensitive to the field rotation, the coupling field

would need to have a linewidth significantly larger than 420 kHz. This could be achieved in two ways, with a very short pulse (1 μs or less) or a very intense RF field (amplitude > 0.84 G). However these conditions are beyond the limits of most current apparatus, so the rotation of the bias field cannot be ignored. Using Eq. (4) we can now determine the total RF transition linewidth

$$\Gamma = \sqrt{\Gamma_{\text{pulse}}^2 + \Gamma_{\text{transit}}^2}. \quad (6)$$

The spatial dependence of the linewidth is shown in Fig. 2 for three different values of Γ_{pulse} .

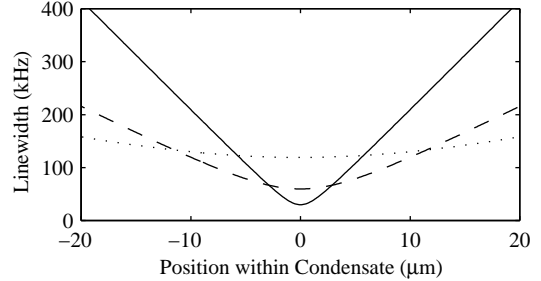


FIG. 2. The total linewidth Γ as a function of position within the condensate for weak RF field and three different pulse lengths: — 20 μs , --- 10 μs , and ··· 5 μs .

There are two regimes that simplify the expression for Γ . The first of these is the case described above, where $\Gamma_{\text{transit}} \ll \Gamma_{\text{pulse}}$, in which case the effects of the rotating field can be ignored (e.g. Figure 2, $\tau_{\text{pulse}} = 5$ μs). The second case is when $\Gamma_{\text{transit}} \gg \Gamma_{\text{pulse}}$ (e.g. in the case of quasi-continuous output coupling). From Eq. (4) we see that the linewidth in this case is approximately linear with radius. However, in our experiments neither of these simple approximations apply and a more complete treatment is required.

We are able to broadly predict the population dynamics of the various m_F states as a function of time with the following simple Rabi cycling model that neglects any kinetic or mean-field effects within the condensate. In an $F = 2$ manifold there are four Rabi frequencies $\Omega_{1\dots 4}$ associated with the RF field, where Ω_1 couples states $|2, 2\rangle \leftrightarrow |2, 1\rangle$, Ω_2 states $|2, 1\rangle \leftrightarrow |2, 0\rangle$, etc. From the Clebsch-Gordan coefficients for the transitions, $\Omega_1 = \Omega_4$, $\Omega_2 = \Omega_3$ and $\sqrt{3}\Omega_1 = \sqrt{2}\Omega_2$ allowing us to define a single $\Omega(t)$ for all transitions

$$\Omega(t) = \frac{g_F \mu_B B_{\text{rf}}(t)}{\sqrt{2}\hbar}. \quad (7)$$

Each RF transition will be detuned an amount $\Delta(r, \theta, t) = \delta(r) \cos(\omega_{\text{TOP}} t + \theta)$ from resonance. The time dependence in Δ is introduced to account for the rotation of the TOP field, and $\delta(r)$ accounts for the effects of ω'_q introduced in Eq. (5). There are also three non-recycling trap loss rates $\gamma_{0\dots -2}$ which account for decay associated with the untrapped states $|2, 0\rangle, |2, -1\rangle$ and $|2, -2\rangle$. Using these parameters we can write the following equation for the population amplitudes of the m_F states $a_{2\dots -2}$

$$\frac{\partial}{\partial t} \begin{pmatrix} a_2 \\ a_1 \\ a_0 \\ a_{-1} \\ a_{-2} \end{pmatrix} = -\frac{i}{2} \begin{bmatrix} 0 & \Omega(t) & 0 & 0 & 0 \\ \Omega(t)^* & 2\Delta(r, \theta, t) & \sqrt{\frac{3}{2}}\Omega(t) & 0 & 0 \\ 0 & \sqrt{\frac{3}{2}}\Omega(t)^* & 4\Delta(r, \theta, t) - i\gamma_0 & \sqrt{\frac{3}{2}}\Omega(t) & 0 \\ 0 & 0 & \sqrt{\frac{3}{2}}\Omega(t)^* & 6\Delta(r, \theta, t) - i\gamma_{-1} & \Omega(t) \\ 0 & 0 & 0 & \Omega(t)^* & 8\Delta(r, \theta, t) - i\gamma_{-2} \end{bmatrix} \begin{pmatrix} a_2 \\ a_1 \\ a_0 \\ a_{-1} \\ a_{-2} \end{pmatrix}. \quad (8)$$

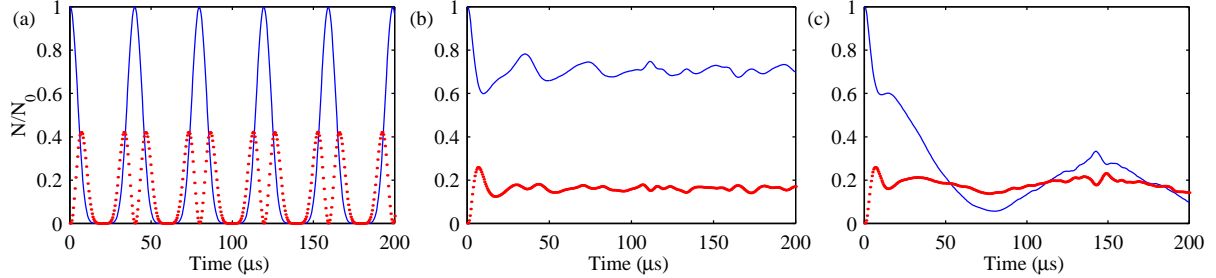


FIG. 3. The populations of the $|2, 2\rangle$ and $|2, 1\rangle$ states as a function of time for $\Omega = 50$ kHz : (a) homogeneous coupling, (b) inhomogeneous coupling with no bias rotation and (c) inhomogeneous coupling with bias field rotation.

For the predictions that follow trap loss is ignored and γ_i 's are set to zero. This is because we estimate that the average time taken for an untrapped atom to be ejected from the trap is approximately 3 ms, so the loss rate γ (≈ 0.3 kHz) is small compared with typical values for Ω and Δ (in the range 10 to 100 kHz).

Figure 3 shows the calculated populations of states $|2, 2\rangle$ and $|2, 1\rangle$ as a function of time for three distinct regimes: (a) strong coupling such that the coupling rate is uniform across the condensate, (b) no bias rotation and weak (and therefore inhomogeneous) coupling across the condensate, and (c) typical experimental conditions of weak coupling with rapid bias field rotation, which introduces temporal variation into the coupling. Unless stated otherwise, to match our experimental conditions we set $\delta(r) = \omega_q' r$ with $\omega_q' = 14$ kHz μm^{-1} , and allow a 1 μs rise and fall time on $B_{\text{rf}}(t)$ which has an amplitude of 72 mG (equivalent to $\Omega \simeq 50$ kHz). To calculate the total population in each state we assume a 3-D Thomas-Fermi distribution of size $30 \mu\text{m} \times 30 \mu\text{m} \times 11 \mu\text{m}$ and integrate over this region.

When the linewidth is significantly larger than the change in transition frequency across the condensate (as in Fig. 3(a)), spatial effects are reduced and the population essentially Rabi cycles between the fully stretched states $|2, 2\rangle$ and $|2, -2\rangle$. For ease of comparison we keep Ω constant across all plots in Fig. 3 and simulate the broad linewidth condition in (a) by reducing the quadrupole field gradient by a factor of 200. For Figs. 3(b) and (c) we return to conditions more relevant to our experiment. For Fig. 3(b), although we have eliminated bias rotation, complex spatial behaviour results since the coupling linewidth is smaller than the Zeeman shift across the condensate. However the decay of Rabi cycling due to large detuning changes across the cloud leads to an equilibrium population distribution that de-

pends only on the pulse linewidth of the transition relative to the Zeeman shift across the condensate. Figure 3(c) has identical parameters to Fig. 3(b) except that the rotation of the bias field has been included, so that the time dependence of Δ is significant. In this case the Rabi cycling is rapidly overwhelmed by a population oscillation at the bias field rotation frequency. This cycling appears only when $r_0\omega_q \gg \Omega \gg \omega_{\text{TOP}}$ where r_0 is the size of the condensate, and can be thought of as a frequency modulation of the coupling field with a beat note at the bias rotation frequency, leading to slow cycling of the population. Along with this cyclic behaviour, our modelling shows that the coupling also introduces interesting small scale spatial structure in the condensate such as shown in Fig. 4.

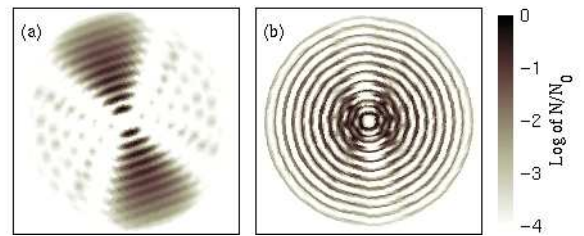


FIG. 4. Spatial structure of the $|2, 2\rangle$ state after RF coupling for (a) 6 μs and (b) 136 μs . The condensates shown are 30 μm across.

The focus of this experimental work is to engineer predetermined relative populations in multi-component condensates. To test the behaviour predicted by the model we first produce Bose condensates in the $|2, 2\rangle$ state as described earlier, and then by varying the duration and power of the RF coupling field we hoped to obtain results similar to those in Fig. 3(b) and (c).

We first considered the case of a relatively short RF pulse, since this minimises the effect of bias field rotation on the coupling surface. To do this we investigated the relative populations of the $|2, 2\rangle$ and $|2, 1\rangle$ states as a function of RF power for a fixed pulse length of $20\ \mu\text{s}$ (compared with a trap rotation period of $143\ \mu\text{s}$). The results of this, along with a simulation, are shown in Fig. 5. It should be noted that there are no free parameters in any of the simulations of relative population.

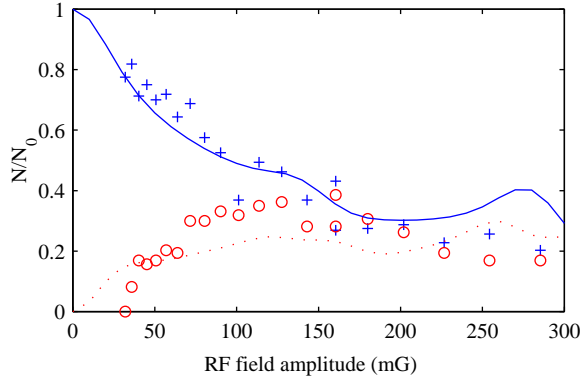


FIG. 5. Populations of the $|2, 2\rangle$ (+) and $|2, 1\rangle$ (o) states as a function of the applied RF magnetic field. The lines are the results of simulations described in the text. The error in the data is of order $\pm 10\%$ of N_0 .

The agreement between the experimental and theoretical results is surprisingly good given the simplistic nature of the model. At a field amplitude of $150\ \text{mG}$ we obtain an approximately equal proportion of atoms in the two trapped states. For comparison we note that this field is significantly larger than that typically required for evaporative cooling. Within the limits of experimental uncertainty, the decrease of the $|2, 2\rangle$ state population with increased RF field behaves as we might expect, whilst the $|2, 1\rangle$ state population appears to grow more rapidly than predicted. The reason for this minor discrepancy may be due to the quadratic Zeeman effect.

Secondly, we considered the case of a weak pulse, since this reduces the effect of power broadening on the linewidth. To do this we investigated the relative populations of the two trapped states as a function of RF pulse length for an RF field amplitude of $72\ \text{mG}$. We varied the pulse length from $10\ \mu\text{s}$ to $1\ \text{ms}$ to cover a range of times relative to the bias field rotation period. Results are shown in Fig. 6. The parameters match those used to generate Fig. 3(c). Rabi cycling is suppressed as expected, and the relative populations rapidly become constant and equal. However, the data does not exhibit the cyclic behaviour of the simulation and we also observe a linear increase in internal energy of the condensate as a function of RF pulse length. We believe that both these observations stem from the spatial structure introduced by the coupling field. There are large phase gradients associated with the predicted spatial structure and these

correspond to increased internal energy. The simulation does not include diffusion effects, and atomic movement on the scale of the spatial structure will tend to average out the slow population cycling at the bias rotation frequency.

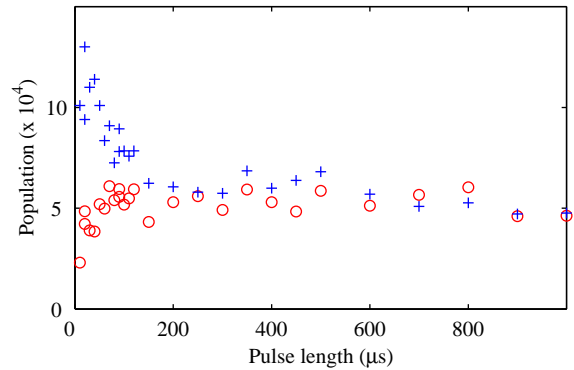


FIG. 6. Populations of the $|2, 2\rangle$ (+) and $|2, 1\rangle$ (o) states as a function of pulse length. The error in the data is of order $\pm 10\%$.

To conclude, we have shown that using an RF field it is possible to engineer multi-state Bose condensates in a TOP trap, and that a simple model predicts the essential features of the condensate behaviour. Our simulations indicate that the coupling process introduces complex spatial features. It may be possible to take advantage of these effects to produce vortex states in TOP traps. This will be the subject of future work at Otago.

We would like to thank Associate Professor R. J. Ballagh and Professor W. J. Sandle for their helpful advice. We are grateful for the financial support of the Royal Society of New Zealand Marsden Fund (contract UOO608), the Foundation for Research, Science and Technology Postdoctoral Fellowship programme (contract UOO524) and the University of Otago Research Committee.

- [1] C. Myatt *et al.*, Phys. Rev. Lett. **78**, 586 (1997).
- [2] M. Matthews *et al.*, Phys. Rev. Lett. **81**, 243 (1998).
- [3] D. Stamper-Kurn *et al.*, Phys. Rev. Lett. **80**, 2027 (1998).
- [4] M.-O. Mewes *et al.*, Phys. Rev. Lett. **78**, 582 (1997).
- [5] I. Bloch, T. W. Hänsch, and T. Esslinger, Phys. Rev. Lett. **82**, 3008 (1999).
- [6] J. Martin *et al.*, J. Phys. B **32**, 3065 (1999).
- [7] E. Hagley *et al.*, Science **283**, 1706 (1999).
- [8] J. Stenger *et al.*, Phys. Rev. Lett. **82**, 4569 (1999).
- [9] B. Anderson and M. Kasevich, Science **282**, 1686 (1998).
- [10] W. Petrich *et al.*, Phys. Rev. Lett. **74**, 3352 (1995).
- [11] R. Loudon, *The Quantum Theory of Light*, 2nd ed. (Oxford University Press, Oxford, 1983), pp.65.